PHYSICAL REVIEW B **80**, 220408(R) (2009)

Observation of ultrafast photoinduced closing and recovery of the spin-density-wave gap in $(TMTSF)_2PF_6$

Shinichi Watanabe,[1] Ryusuke Kondo,[2] Seiichi Kagoshima,[2] and Ryo Shimano[1,*]
[1]*Department of Physics, The University of Tokyo, 7-3-1 Hongo, Bunkyo-ku, Tokyo 113-0033, Japan*
[2]*Department of Basic Science, The University of Tokyo, 3-8-1 Komaba, Meguro-ku, Tokyo 153-8902, Japan*
(Received 13 October 2009; published 17 December 2009)

Photoexcited dynamics of a spin-density-wave (SDW) state in an organic linear-chain compound bis-(tetramethyl-tetraselenafulvalene)hexafluorophosphate, $(TMTSF)_2PF_6$, is investigated by optical pump and terahertz probe experiments. After the ultrashort laser-pulse excitation, a sudden closing followed by a recovery of the SDW gap is clearly observed in the far-infrared spectrum. The recovery time is found to diverge toward the phase-transition temperature, T_{SDW}, while the gap remains open at T_{SDW}. The observed critical slowing down behavior is interpreted in terms of three-dimensional fluctuation which enlarges near the phase-transition temperature.

DOI: 10.1103/PhysRevB.80.220408 PACS number(s): 75.30.Fv, 64.60.Ht, 71.30.+h, 78.30.Jw

The interplay between different ordered phases, such as superconductivity (SC) and charge or spin-density-wave (CDW or SDW) orders, is one of the central interests in condensed-matter physics.[1] Both CDW and SDW instabilities could develop in the presence of Fermi-surface nesting, while such instabilities may compete with other possible orderings, which provides a rich variety of ground states in the phase diagram. The model example is a quasi-one-dimensional (1D) organic conductor $(TMTSF)_2PF_6$ [TMTSF denotes bis-tetramethyl-tetraselenafulvalene], where SC and the SDW ground states are neighboring each other in its pressure-temperature phase diagram.[2] The proximity of SDW and SC phases indicates that SC pairing is mediated by the exchange of spin fluctuations.[3] Photoexcitation in these symmetry-broken ground states is a very exciting phenomenon, which could result in a drastic modification of the electronic properties, as exemplified by the photoinduced phase transition from SC[4] and CDW[5] to normal metals, or photoinduced creep of CDW collective motion.[6] Quasiparticle (QP) dynamics has also been elucidated in CDW systems[7,8] and in high-temperature superconductors[9,10] through the femtosecond pump and probe spectroscopy. In contrast to these intensive studies in SC and CDW systems, however, only a few examples have been reported on the photoexcited dynamics in SDW systems,[11] and the photoinduced dynamics of spin fluctuation in SDW system remains an open issue.

Here, we investigate the photoexcited dynamics of the prototypical SDW system in $(TMTSF)_2PF_6$. To investigate the temporal evolution of SDW order after the photoexcitation, we directly observe the SDW gap in the optical conductivity spectra by the terahertz time-domain spectroscopy (THz-TDS). The recovery dynamics of the SDW order shows the three-dimensional (3D)-like critical Ginzburg-Landau fluctuation behavior in a wide range of temperatures near the SDW phase-transition temperature T_{SDW}, reflecting the anisotropic coherence length inherent to quasi-1D nature of the electronic system.

The single crystals of $(TMTSF)_2PF_6$ are grown by electrochemical oxidation, with the typical size of 4 mm in the a axis and 0.7 mm in the b axis, respectively, where the a axis is the electronic one-dimensional axis.[12] b' axis is defined as perpendicular to the a axis which is slightly tilted from the crystallographic b axis because the crystal is triclinic. The sample is mounted on a copper plate glued by the epoxy resin Stycast 1266 with the a-b plane on its surface and embedded in a cryostat. The measurement is performed by using an output from a 1 kHz regenerative amplifier as a light source for the optical pump and for the THz-TDS measurement. The pulse width of the laser is 90 fs and the center wavelength is 800 nm (1.55 eV). A diffraction-limited spatial resolution is achieved by the THz-TDS, making it possible to measure the typically small samples, and the experimental details are described elsewhere.[13] The polarization of the terahertz electric field is set to the b' axis.

Figure 1(a) shows the temperature dependence of the conductivity spectra retrieved from the complex reflectivity determined by THz-TDS. Please note that the spectra are normalized by the metallic conductivity at 15 K. By measuring the reflectivity and the phase change with respect to the value at the metallic state above T_{SDW}, we could avoid the phase uncertainty problem between the sample and the reference mirror peculiar to reflection-type THz-TDS measurements.[13] We use the Drude parameters of the metallic phase in Ref. 14 in the analysis and plot the normalized conductivity comparing the two reflectivity spectra at different temperatures. A clear suppression of the conductivity in the low-frequency range and a slight increase in the higher frequency side can be seen upon cooling, indicating the opening of the SDW gap. Figure 1(b) shows the temperature dependence of the value of the SDW gap estimated from the photon energy below which the optical conductivity becomes smaller than the metallic one at 15 K as indicated by arrows in Fig. 1(a). The value of the gap at each temperature is normalized by that at $T=4\ \mathrm{K} \ll T_{SDW}$ and corresponds to the amplitude of the SDW order parameter. Also shown is the SDW gap extracted from the FTIR spectroscopy reported in Ref. 14. The good agreement ensures the validity of THz-TDS in obtaining the optical conductivity spectrum without resorting to the Kramers-Krönig analysis for typically small organic crystals (0.7 mm in the present case) whose width is only twice the wavelength of the probe terahertz beam. As previously pointed in Refs. 14 and 15, the SDW gap opens

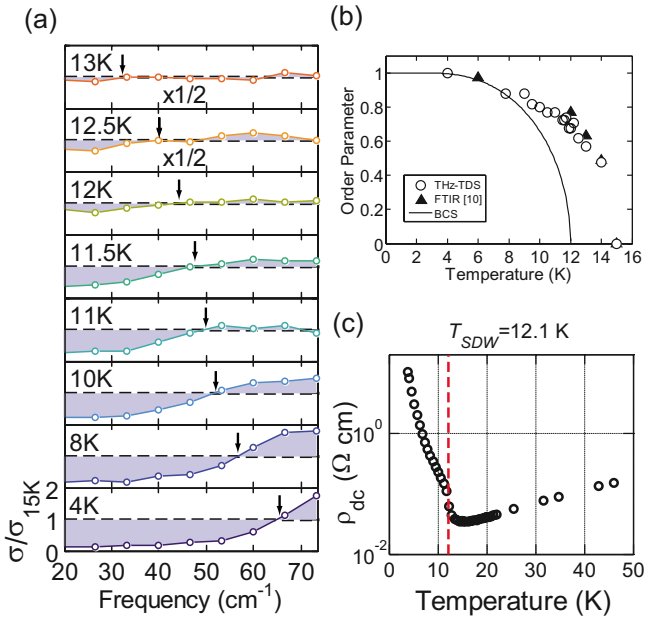

FIG. 1. (Color online) (a) Temperature dependence of the conductivity spectra of $(TMTSF)_2PF_6$. Each spectrum is normalized by the metallic conductivity spectrum at 15 K reported in Ref. 14. Polarization of the probe terahertz electric field is set to the b'-axis. Lines are guides to the eye. (b) Temperature dependence of the SDW order parameter as evaluated from arrows in Fig. 1(a). The data obtained by FTIR measurements in Ref. 14 are also plotted. Theoretical curve calculated by the BCS theory is also shown. (c) Temperature dependence of the dc resistivity, where the metal-to-insulator transition is clearly observed at 12.1 K.

already at temperatures approximately 2 K above T_{SDW} which is determined from the dc resistivity measurement shown in Fig. 1(c) and could be related to the pseudogap due to the three-dimensional fluctuation effects. Please note that the measured dc resistivity is much larger than the value reported in Ref. 16 due to the formation of cracks during the cooling process, while the terahertz optical responses do not change during the repeated heat cycle between 4 K and room temperature for more than 30 times.

We next investigate the photoinduced changes of the conductivity spectrum. The pump pulse is loosely focused onto the sample with a spot size of ~1.5 mm in diameter, which is sufficiently wider compared to the tightly focused terahertz probe beam (less than 0.7 mm in diameter depending on the wavelength) so that the uniform excitation condition is achieved. Figure 2(a) shows the conductivity spectra at 3 ps after the excitation with the indicated excitation-power densities. The lattice temperature is kept at 4 K. Apparently, the SDW gap diminishes as the excitation-power density increases and almost closes around 27.4 $\mu J/cm^2$. The observed excitation-power dependence of the conductivity spectra is very similar to the temperature dependence shown in Fig. 1(a). This similarity suggests that the electronic distribution described as an effective temperature T^*_{ini} is established within 3 ps after the laser-pulse excitation, thereby inducing the ultrafast closing of the SDW gap.

Figure 2(b) describes the pump and probe delay dependence of the conductivity spectra for 13.7 $\mu J/cm^2$

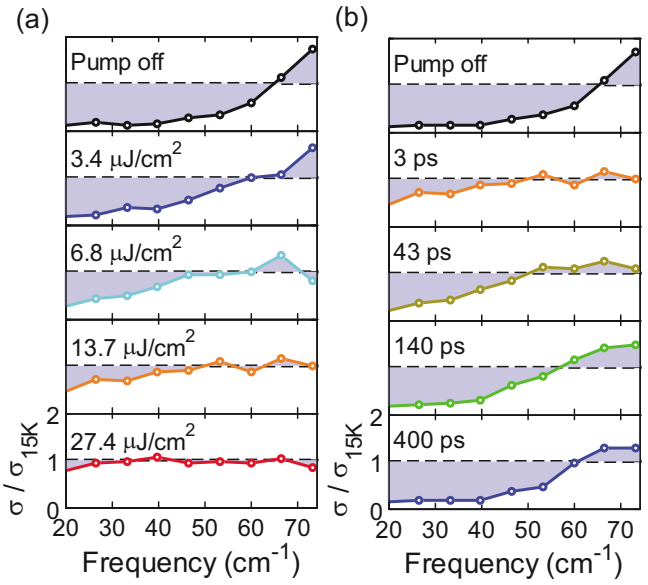

FIG. 2. (Color online) Ultrafast laser-pulse induced conductivity spectra of $(TMTSF)_2PF_6$ at T=4 K. (a) Excitation-power dependence at 3 ps after the excitation. (b) Temporal evolution of the spectra at 13.7 $\mu J/cm^2$ excitation-power density.

excitation-power density and shows that the SDW gap recovers gradually from 3 to 400 ps. By comparing the conductivity spectra in Fig. 2(b) with those in Fig. 1(a), we estimate the effective temperature T^* of the electronic system in each delay time. We observe that T^* increases within 3 ps after the photoexcitation, followed by a gradual decrease, and finally after 400 ps, the spectral shape becomes almost similar to that without the excitation, although a slight reduction in the gap energy is discerned. Figure 3 summarizes the excitation-power dependence of the effective temperature at several delay times. We also plot the local thermal equilibrium temperature, T_{eq}, assuming that all the absorbed pump-laser power contributes to the increase in the sample temperature, by using the reported values of specific heat,[17] reflectivity, and absorption coefficient for the pump pulse.[18] Clearly, the estimated effective temperature just after the excitation is far

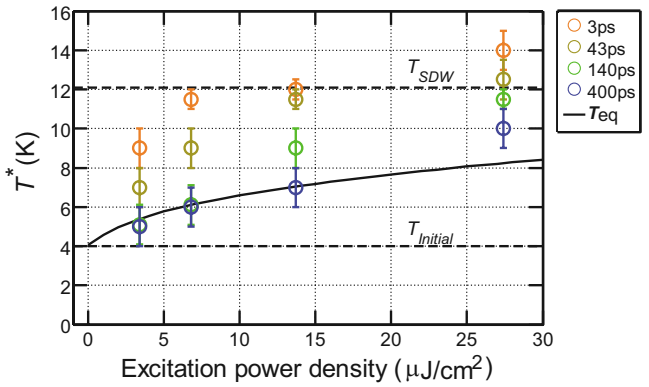

FIG. 3. (Color online) Excitation-power and time-dependent electron temperature T^* (circles) estimated by comparing the conductivity spectra with those of the temperature dependence in Fig. 1(a). The local thermal equilibrium temperature T_{eq} (line) is estimated from the specific-heat value as described in the text.

above T_{eq}, and it approaches to T_{eq} in the time scale of ~400 ps. These results suggest that the observed temporal change of the spectra is caused by the instantaneously produced nonequilibrium electronic distribution which closes the SDW gap, followed by the subsequent relaxation. T_{eq} is considered to decrease in a much longer time scale because the thermal diffusion coefficient is small enough,[19] while it reaches to the bath temperature (4 K) within the repetition rate of the laser pulse (1 ms) since no changes are observed in the conductivity spectra before the laser-pulse excitation.

The closing and recovery mechanism of the spectral gap by the optically induced nonequilibrium QPs distribution has been studied theoretically[20,21] and experimentally[22] in superconductors, and theoretically in SDW systems[23] based on the BCS theory. In the present case, the intramolecular (highest occupied molecular orbital to lowest unoccupied molecular orbital) excitations caused by the pump-laser pulse are considered to relax rapidly, thereby yielding a large number of high-energy QPs whose energies finally settle close to the gap energy Δ where the density of states is large. Through the frequent emission or absorption of the phonons with the energy greater than 2Δ that occurs during the initial relaxation process of QPs, QPs and high-frequency phonons (with energy $\hbar\omega > 2\Delta$) are considered to form a near-steady-state distribution, whose temperature can be described as T^*_{ini}. Accordingly, the single-particle gap closes to the value represented as $\Delta(T^*_{ini})$[21] in the time scale less than 3 ps in the present case of $(TMTSF)_2PF_6$. On the other hand, the phonons with energy $\hbar\omega < 2\Delta$ would stay in the same energy distribution as the one before the laser-pulse excitation. Accordingly, the QPs near the gap are prevented from the relaxation across the gap because of the small numbers of low-energy phonons with $\hbar\omega < 2\Delta$, so-called phonon-bottleneck effect.[24] The final QPs relaxation step across the gap accomplishes by the phonon-phonon scattering which induces energy transfer from high-frequency phonons with $\hbar\omega > 2\Delta$ to phonons with $\hbar\omega < 2\Delta$, and the local thermal equilibrium condition is then achieved. As a result, the temperature of the electronic system decreases, and accordingly the single-particle gap opens again. The QPs relaxation model described above is considered to be valid when T^* is far below T_{SDW}, where the SDW long-range order well develops.

Figure 4(a) shows the temperature dependence of the temporal evolution of the terahertz reflectivity change. Here, we plot the peak amplitude of the reflected terahertz electric field which we consider well represents the SDW gap behavior because the peak of the reflected pulse monotonously decreases when the gap opens. The excitation-power density is kept at low level of 2 $\mu J/cm^2$ to suppress the final local equilibrium temperature T_{eq} as low as possible, which is estimated to be only ~0.1 K higher than the bath temperature T when $T > 10$ K. In all the curves, the reflectivity sharply increases at $t=0$ indicating that the SDW gap closes instantaneously. While the recovery time is nearly constant from 4 to ~10 K, it dramatically increases above ~10 K. Near T_{SDW}, we cannot detect any decay of the reflectivity during our measurement time scale (up to 400 ps). The experimentally observed decay curves in Fig. 4(a) can be well fitted by a single exponential function with a constant term, $\Delta E(t) = A\exp(-t/\tau) + B$, where the first term represents the gap recovery and B represents much slower dynamics presumably due to the heating of the sample. The ratio B/A is quite small at the weak excitation density of 2 $\mu J/cm^2$ and is consistent with the small temperature increase of $T_{eq} \sim 0.1$ K. Figures 4(b) and 4(c) show the temperature dependence of the gap recovery time τ deduced from the fitting. Apparently, τ diverges toward T_{SDW} and scales as $\tau \propto (1 - T/T_{SDW})^{-\gamma}$, with $\gamma = 1.2 \pm 0.3$.

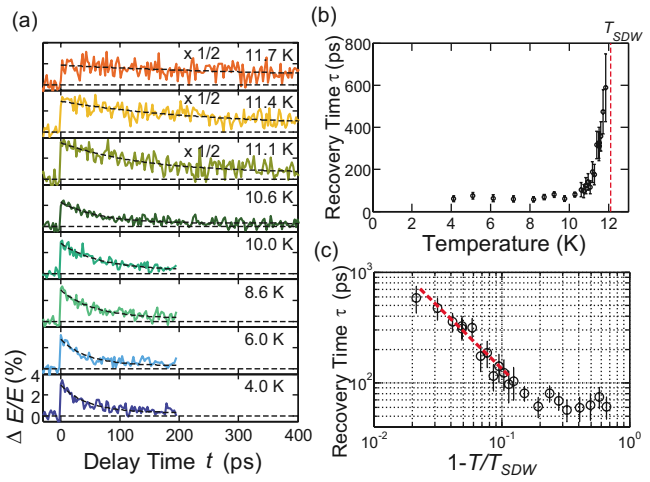

FIG. 4. (Color online) (a) Temporal evolution of the photoinduced terahertz reflectivity change $\Delta E/E$ at the indicated temperatures. Every curve can be well fitted by the relation $\Delta E/E = A\exp(-t/\tau) + B$ (dotted lines), where the origins of the two components are described in the text. (b) Temperature dependence of the relaxation time τ. The error bars originate from the uncertainty in the determination of the constant term B in the fitting process. (c) The logarithmic plot of the data in (b) as a function of $(1 - T/T_{SDW})$. Dashed line shows the fitting with the power law, $\tau \propto (1 - T/T_{SDW})^{-\gamma}$ with $\gamma = 1.2(\pm 0.3)$.

One possible mechanism to explain the observed divergence of τ may be the phonon-bottleneck effect, as often described in superconductors.[10,24] In this mechanism, the QP relaxation time across the single-particle gap is proportional to $1/\Delta(T)$ in the low pump fluence limit, and accordingly it diverges toward the phase-transition temperature where Δ approaches to zero. However as confirmed in Fig. 1(b), Δ remains open at T_{SDW}, which contradicts with the above interpretation. The discrepancy can be attributed to the critical fluctuation effects near the phase-transition temperature T_{SDW}. In $(TMTSF)_2PF_6$, the anisotropy of the coherence length inherent to the quasi-1D electronic system significantly enlarges the Ginzburg critical width ζ_T which gives the temperature region where the three-dimensional fluctuation effects become dominant in the units of $|1 - T/T_{SDW}|$, making a contrast with the 3D BCS superconductors. The calorimetric measurement[25] gives the estimation of ζ_T about 0.1 which shows an agreement with our temperature range in Fig. 4(c) where the power-law divergence of τ is observed. In the critical regime with the long-range fluctuation, the QP relaxation across the single-particle gap becomes less relevant. Instead, the relaxation process would reflect the thermalization of the optically induced fluctuation, presumably the low-energy collective excitations such as magnons. The relaxation dynamics for such collective excitation can be

characterized by the dynamical scaling relation $\tau \propto |1 - T/T_{SDW}|^{-z\nu}$ near the critical point, where $z \sim 1.5$[26] and $\nu \sim 0.7$,[27] respectively, and thus $z\nu \sim 1.05$ for the 3D Heisenberg antiferromagnetic model. The critical exponent of $\gamma = 1.2 \pm 0.3$ observed in the experiments is close to this value, indicating the 3D nature of the SDW order. A similar critical behavior described by the 3D Heisenberg antiferromagnetic model has been also observed in the line width broadening of the electron-spin-resonance signal.[28] The pseudogap behavior observed above T_{SDW} in Fig. 1(b) would also be the consequence of the fluctuation and would reflect the development of short-range coherence above T_{SDW}.[14,15] Proton nuclear magnetic resonance[29] and muon-spin-rotation experiments[30] show that the SDW order well develops at T_{SDW}, which is consistent with the development of the short-range coherence above T_{SDW}.

In summary, our results show directly the dynamics of the SDW gap closing and recovery in $(TMTSF)_2PF_6$ after the instantaneous photoexcitation. At electronic temperature far below T_{SDW}, the dynamics can be described by the relaxation of excess QPs injected by the optical pulse as predicted in the BCS mean-field theory. However in the vicinity of T_{SDW} where fluctuation effect becomes important, the relaxation rate of the order parameter is described by the dynamical scaling relation or the critical slowing down, in accordance with the 3D Heisenberg antiferromagnetic model. Importantly, the relaxation dynamics of the photoinduced fluctuation near T_{SDW} is governed by long-range fluctuation which diverges at T_{SDW}, while the gap in the conductivity spectrum develops already above T_{SDW} reflecting the short-range coherence. Such direct access to the dynamics of QPs or collective excitations enabled by THz-TDS would be promising for the further investigation on the density wave states, the superconducting states, and other symmetry-broken ground states in low-dimensional electronic systems and also for the optical control of the electronic phases.

This work was partially supported by a Grant-in-Aid for Scientific Research on Innovative Areas 20110005 and by that for Young Scientists (B) No. 20740170 from the Ministry of Education, Culture, Sports, Science and Technology, Japan.

*shimano@phys.s.u-tokyo.ac.jp

[1] A. M. Gabovich, A. I. Voitenko, and M. Ausloos, Phys. Rep. **367**, 583 (2002).
[2] D. Jérome, Science **252**, 1509 (1991).
[3] V. J. Emery, Synth. Met. **13**, 21 (1986).
[4] L. R. Testardi, Phys. Rev. B **4**, 2189 (1971).
[5] A. Tomeljak, H. Schäfer, D. Städter, M. Beyer, K. Biljakovic, and J. Demsar, Phys. Rev. Lett. **102**, 066404 (2009).
[6] N. Ogawa, A. Shiraga, R. Kondo, S. Kagoshima, and K. Miyano, Phys. Rev. Lett. **87**, 256401 (2001).
[7] J. Demsar, K. Biljakovic, and D. Mihailović, Phys. Rev. Lett. **83**, 800 (1999).
[8] K. Shimatake, Y. Toda, and S. Tanda, Phys. Rev. B **73**, 153403 (2006).
[9] J. Demsar, B. Podobnik, V. V. Kabanov, T. Wolf, and D. Mihailovic, Phys. Rev. Lett. **82**, 4918 (1999).
[10] V. V. Kabanov, J. Demsar, B. Podobnik, and D. Mihailovic, Phys. Rev. B **59**, 1497 (1999).
[11] E. E. M. Chia, J. X. Zhu, H. J. Lee, N. Hur, N. O. Moreno, E. D. Bauer, T. Durakiewicz, R. D. Averitt, J. L. Sarrao, and A. J. Taylor, Phys. Rev. B **74**, 140409(R) (2006).
[12] S. Kagoshima, Y. Saso, M. Maesato, R. Kondo, and T. Hasegawa, Solid State Commun. **110**, 479 (1999).
[13] S. Watanabe, R. Kondo, S. Kagoshima, R. Shimano, Phys. Status Solidi B **245**, 2688 (2008).
[14] V. Vescoli, L. Degiorgi, M. Dressel, A. Schwartz, W. Henderson, B. Alavi, G. Grüner, J. Brinckmann, and A. Virosztek, Phys. Rev. B **60**, 8019 (1999).
[15] L. Degiorgi, M. Dressel, A. Schwartz, B. Alavi, and G. Grüner, Phys. Rev. Lett. **76**, 3838 (1996).
[16] K. Bechgaard, C. S. Jacobsen, K. Mortensen, H. J. Pedersen, and N. Thorup, Solid State Commun. **33**, 1119 (1980).
[17] H. Yang, J. C. Lasjaunias, and P. Monceau, J. Phys.: Condens. Matter **11**, 5083 (1999).
[18] M. Dressel, A. Schwartz, G. Grüner, and L. Degiorgi, Phys. Rev. Lett. **77**, 398 (1996).
[19] D. Djurek, D. Jérome, and K. Bechgaard, J. Phys. C **17**, 4179 (1984).
[20] C. S. Owen and D. J. Scalapino, Phys. Rev. Lett. **28**, 1559 (1972).
[21] W. H. Parker, Phys. Rev. B **12**, 3667 (1975).
[22] G. L. Carr, R. P. S. M. Lobo, J. LaVeigne, D. H. Reitze, and D. B. Tanner, Phys. Rev. Lett. **85**, 3001 (2000).
[23] E. M. Conwell and N. C. Banik, Phys. Rev. B **26**, 530 (1982).
[24] A. Rothwarf and B. N. Taylor, Phys. Rev. Lett. **19**, 27 (1967).
[25] J. Coroneus, B. Alavi, and S. E. Brown, Phys. Rev. Lett. **70**, 2332 (1993).
[26] P. C. Hohenberg and B. I. Halperin, Rev. Mod. Phys. **49**, 435 (1977).
[27] G. S. Rushbrooke, G. A. Baker, and P. J. Wood, in *Phase Transition and Critical Phenomena*, edited by C. Domb and M. S. Green (Academic, New York, 1974), Vol. 3, p. 245.
[28] M. Dumm, A. Loidl, B. Alavi, K. P. Starkey, L. K. Montgomery, and M. Dressel, Phys. Rev. B **62**, 6512 (2000).
[29] T. Takahashi, H. Kawamura, T. Ohyama, Y. Maniwa, K. Murata, G. Saito, J. Phys. Soc. Jpn. **58**, 703 (1989).
[30] L. P. Le, A. Keren, G. M. Luke, B. J. Sternlieb, W. D. Wu, Y. J. Uemura, J. H. Brewer, T. M. Riseman, R. V. Upasani, L. Y. Chiang, W. Kang, P. M. Chaikin, T. Csiba, and G. Grüner, Phys. Rev. B **48**, 7284 (1993).